r_m = radius to point of maximum local velocity, ft.

u = temporal mean local velocity of fluid at radius r, ft./sec.

u_m = maximum temporal mean local velocity of fluid at radius r_m, ft./sec.

V = bulk average linear velocity of fluid, ft./sec.

μ = viscosity of fluid, lb.-mass/(sec.) (ft.)

ρ = density of fluid, lb.-mass/cu. ft.

τ_1 = skin friction at core, lb.-force/sq. ft.

τ_2 = skin friction at outer wall, lb.-force/sq. ft.

LITERATURE CITED

1. Knudsen, J. G., and D. L. Katz, *Proc. Midwestern Conference on Fluid Dynamics*, 1st Conference, No. 2, 175 (1950).
2. Koch, R., and K. Feind, *Chemie Ingenieur Technik*, **30**, 577 (1958).
3. Lamb, Horace, "Hydrodynamics," 5 ed., p. 555, Cambridge Univ. Press, London, England (1924).
4. Rothfus, R. R., C. C. Monrad, and V. E. Senecal, *Ind. Eng. Chem.*, **42**, 2511 (1950).
5. Rothfus, R. R., C. C. Monrad, K. G. Sikchi, and W. J. Heideger, *ibid.*, **47**, 913 (1955).
6. Rothfus, R. R., J. E. Walker, and G. A. Whan, *A.I.Ch.E. Journal*, **4**, 240 (1958).
7. Stanton, T. E., D. Marshall, and C. N. Bryant, *Proc. Roy. Soc. (London)*, **A85**, 366 (1911).
8. Walker, J. E., Ph.D. thesis, Carnegie Institute of Technology, Pittsburgh, Pennsylvania (1957).
9. ———, and R. R. Rothfus, *A.I.Ch.E. Journal*, **5**, 51 (1959).
10. Walker, J. E., G. A. Whan, and R. R. Rothfus, *ibid.*, **3**, 484 (1957).

Manuscript received September 20, 1960; revision received June 27, 1961; paper accepted June 30, 1961.

Heat Transfer from the Surface of a Steam Bubble in Turbulent Subcooled Liquid Stream

S. G. BANKOFF and J. P. MASON

Northwestern University, Evanston, Illinois

Turbulent heat transfer coefficients have been measured at the surface of single bubbles formed by injecting steam into a subcooled water stream at atmospheric pressure. Depending upon the steam flow rate (0.4 to 1.5 g./min), the water temperature (80° to 180°F.), and the water velocity (0.9 to 7.2 ft./sec.) the bubbles ranged from small, smooth, ellipsoidal bubbles, similar to those observed in highly subcooled nucleate boiling, to large, irregular bubbles which oscillated in size. The bubble frequencies were in the range 200 to 2,500 cycles/sec. and the surface heat transfer coefficients 13,000 to 320,000 B.t.u./(hr.) (sq. ft.) (°F.). Because of these exceptionally high heat transfer coefficients a significant fraction of the total heat flow in Gunther's subcooled boiling experiments is estimated to be attributable to latent heat transport.

A problem of considerable importance in the study of the mechanism of nucleate boiling transfer is whether an appreciable fraction of the total heat flux flows in the form of latent heat through the two-phase wall boundary layer into the turbulent core. Gunther and Kreith (*1, 2*) and also Rohsenow and Clark (*3*) measured the rate of production of vapor in subcooled nucleate boiling of water at atmospheric pressure and noted that only 1 to 2% of the total heat flux in subcooled nucleate boiling could be accounted for by the latent heat content of this vapor. Gunther and Kreith further considered the possibility of simultaneous vaporization of hot liquid at the base and condensation at the top of the bubble and showed that this would not greatly increase the rate of latent heat transport, providing that the bubble is surrounded by a stagnant liquid film. The tentative conclusions which were drawn were that the rate of latent heat transport was negligible, the bubbles acting principally as small stirring devices. Essentially this would imply that it would make no difference whether the bubbles were filled with vapor or with inert gas, and indeed it has been shown by Beatty and co-workers (*4*) that nonboiling heat transfer coefficients are increased by a factor of 2 or 3 by generating inert gas bubbles at the heating surface. However the heat fluxes produced, even at the highest generation rate of inert gas bubbles, were in the range of the lower limit of nucleate boiling. One may therefore speculate that, although the stirring effect dominates relatively low heat fluxes, another mechanism may become important as the bubbles become more closely packed and the upper limit of nucleate boiling is approached. Bankoff (*5*), in a study of the mechanism of subcooled boiling, noted several pieces of indirect evidence which indicated that latent heat transport was not insignificant, especially near the upper limit of nucleate boiling, and concluded that the relative importance of stirring and latent heat transport effects needed further study. It was suggested that turbulent heat transfer coefficients at the surface of a rapidly growing bubble might be one or more orders of magnitude greater than the heat transfer coefficient to a bubble surrounded by a liquid in laminar radial flow with no tangential components. The present work, which is a study of turbulent heat transfer coefficients to rapidly growing and collapsing bubbles formed at the surface of a horizontal plate in the presence of a subcooled liquid stream, was undertaken to provide further information on this subject.

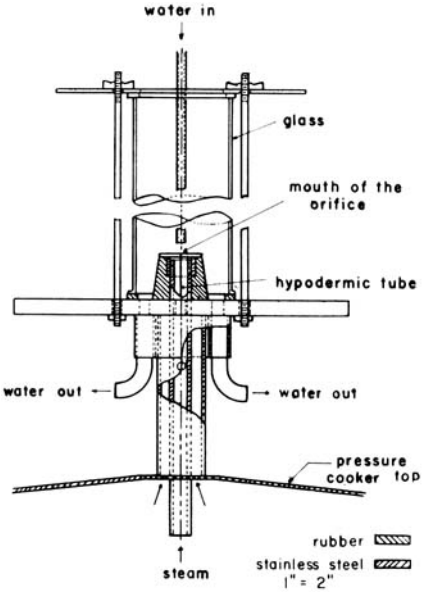

Fig. 1. Bubble heat transfer cell.

PREVIOUS WORK

Although a number of studies of heat and mass transfer to solid spheres and droplets have been made, no previous study has come to the attention of the authors of heat transfer to

rapidly growing and collapsing bubbles. Among the large number of previous studies of turbulent transport to solid spheres or to droplets the investigations of Frossling (6), Kramer (7), Maisel and Sherwood (8), Ranz and Marshall (9), and Hsu and Sage (10) are prominent. In general the Nusselt number for turbulent heat transfer is correlated in terms of Reynolds number and Prandtl number, or Peclet number.

DESCRIPTION OF EQUIPMENT

The bubble heat transfer cell, Figure 1, was essentially a device for bleeding dry saturated steam through a pinhole orifice into a liquid stream in order to form a rapidly growing and collapsing bubble. A submerged jet of water, whose temperature and velocity were controlled parameters, was projected downwards onto the bubble. The bubble outlines were recorded by high-speed photography, and the average steam flow rate was determined by means of a calibrated orifice. From these measurements an average heat transfer coefficient was calculated for ten or more bubbles at each set of conditions.

The orifice plate, consisting of a brass plate ⅞ in. in diameter with a length of hypodermic tubing pressed and silver soldered into a hole in its center, was affixed to the top of a small steam chamber mounted on a 4-qt. pressure cooker. The objective of this design was to obtain a metered stream of dry, saturated steam from the orifice.

The cell consisted of a 2⅜ in. I.D. Pyrex glass tube clamped to the stainless plate with soft rubber gasketing. Distilled, degassed water was brought into the cell through a ¼ in. I.D. glass tube positioned directly above the steam orifice. The water was drained from the cell through four equally spaced ¼-in. holes in the steel plate, whose flow resistance was sufficient so that the discharge rates through each of the holes were substantially equal. The water was circulated at 0 to 1 gal./min. by means of a pump through a coil type of heat exchanger, whereby the inlet water temperature could be varied from 50° to 200°F. The water flow rate was measured by means of an orifice and a 20-in. mercury manometer (Figure 2). The height of the water in the cell was ordinarily maintained at 3 in.

The pressure cooker was insulated by a 1-in. thickness of asbestos enclosed in a brass sheath. A cooling coil was also enclosed in the sheath for rapid control of the pressure. The heat was supplied by a 660-w. hot plate regulated by a 115-v. variac transformer. The vapor pressure was measured by a 50-in. carbon tetrachloride water manometer, or a 36-in. mercury water manometer.

The orifice was calibrated by condensing the steam, followed by direct determination of the weight rate of flow of the condensate. Because of the range of steam flow rates it was desirable to use two different orifices, which helped minimize bubble distortion due to the momentum of the issuing steam. Orifice 1 was constructed from a 1½ in. length of 0.0195 in. I.D. stainless steel hypodermic tubing and was used at steam flow rates of 0.37 to 1.0 g./min. Orifice 2 was constructed from a ⅜ in. length of the same tubing silver soldered to an expansion section 1 in. long with an exit diameter of 0.068 in. and was used at steam flow rates of 1.0 to 1.5 g./min.

The mechanical energy loss, due to entrance, frictional, and exit effects in the hypodermic tubing, is given approximately by Equation (1):

$$\Delta P_1 = \frac{\rho_s v_s^2}{2}\left[\frac{4 f L_t}{D_t} + 1.5\right] \quad (1)$$

The inertial pressure in bubble growth is given by

$$\Delta P_2 = \frac{3}{2}\rho_L \dot{R}^2 + \rho_L R \ddot{R} \quad (2)$$

the dots denote first and second derivatives with respect to time. The first term is always positive, while the second term is typically negative and nonnegligible. In order to obtain an upper bound for the inertial bubble pressure the positive term only was considered.

The irreversible mechanical energy losses were calculated to be typically 1.57 lb./sq. in. at a steam flow rate of 1.0 g./min., 0.73 lb./sq. in. at 0.6 g./min., and 0.40 lb./sq. in. at 0.4 g./min., while the upper bounds for the inertial pressure within the bubble were 1.15, 0.42, and 0.37 lb./sq. in. respectively. Hence fluctuations in steam flow due to the variation of inertial pressure in the bubble were small, except possibly at the lowest flow rates.

At the beginning of a run the vapor generator was filled with water, and the reservoir in the water circulation system was flushed and refilled. The circulating water was boiled to avoid interference by precipitation of gas bubbles. The vapor generator was then heated at maximum rate until it reached the boiling temperature of the water and was maintained there for at least 1 hr. in order to bleed any air out of the system. When steady, or very nearly steady, conditions were obtained, the pressure drop across the steam orifice, the circuating water flow rate and temperature, the height of the water level, the barometric pressure, and the room temperature were recorded. The lights were then turned on and the camera started, photographing a sequence of bubbles.

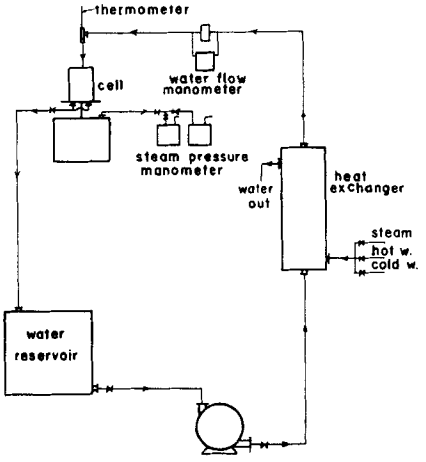

Fig. 2. Flow system.

PHOTOGRAPHIC EQUIPMENT

A motion picture camera with 2-, 4-, 6-in. focal length lenses was used in this work. The camera speed could be regulated from 150 to 8,000 frames/sec. by means of a goose control unit. A pulse generator was used to get accurate timing marks at 100 or 1,000 cycles/sec. By means of extension tubes it was possible to get image magnifications of 1.5 on the film, which were then increased by a factor of 20 by projecting the negatives onto a sheet of quadrille-ruled paper. A high-power magnifying eyepiece was used for more exact focussing at high magnification. Black and white negative film was used. The camera was mounted on a small track fitted with a fine adjustment screw, which is imperative for focussing at high magnifications. The track itself was mounted on a tripod.

Several lighting arrangements with 500-w. photospot bulbs were tried. It is important to eliminate spurious reflections from the bubble surfaces, which mask the true outlines of the bubble. It was found, after a good deal of experimentation, that the best arrangement was to silhouette the bubble by means of a ground-glass screen placed behind it, with a 500-w. bulb pointing directly into the camera through the screen. By force-developing the negative film it was possible to obtain high-contrast silhouettes free from internal reflections often encountered in bubble photography.

ANALYSIS OF DATA

The film was projected, frame by frame, upon a piece of quadrille-ruled paper, and the maximum bubble width and height were recorded for each frame. The total magnification was obtained either by substituting an object of known dimensions in place of the bubble in a trial exposure of film or by measuring the dimensions of the inlet water tube when it was visible.

It was assumed, in analyzing the data, that the vapor within the bubble always consists of dry, saturated steam at atmospheric pressure. It can be easily shown that the surface tension and vapor inertia effects introduce negligible corrections to this assumption.

The mean surface area of a series of bubbles was approximated by obtaining the mean of the measured bubble height and maximum width for one hundred consecutive frames. This mean was weighted for those frames where the bubble was not visible by assuming the meniscus to be a hemisphere whose area was equal to the average cross-sectional area of the orifice. The mean bubble surface area and volume were

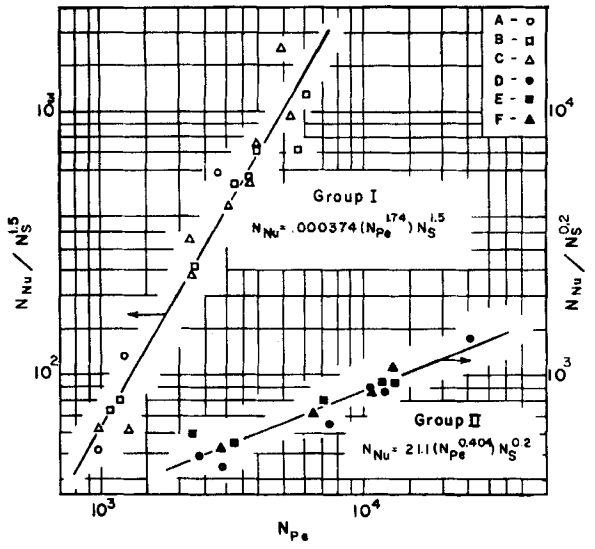

Fig. 3. Ellipsoidal bubbles that completely collapse, Group I—smooth, Group II—irregular.

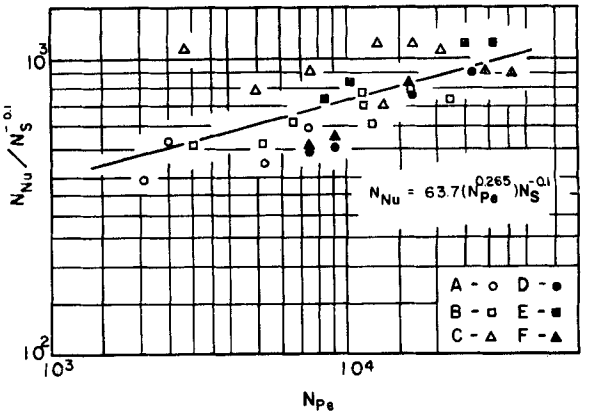

Fig. 4. Group III, irregular bubbles that do not completely collapse.

computed from the properties of a semiellipsoid of revolution having the same mean height and width as the bubble. The characteristic length for formulation of Nusselt and Peclet numbers was chosen to be the diameter of the hemisphere having the same volume as the mean semiellipsoid. The mean bubble wall velocity was computed as the ratio of the characteristic length to the mean bubble period. For bubbles which did not collapse completely the difference between the average maximum and minimum bubble heights was used in calculating the mean bubble wall velocity.

RESULTS

The following ranges of system variables were used: steam flow rate, 0.40 to 1.5 g./min.; water temperature, 80° to 180°F.; water velocity, 0.88 to 7.2 ft./sec. It was found that there was a large variation in bubble shape depending upon the water velocity and temperature and the steam flow rate. Three distinct groups of bubbles could be distinguished.

Group I: Ellipsoidal Bubbles, Smooth Surface

At the lower steam flow rates and water temperatures the bubble first appeared as a very small, rapidly growing hemisphere, which elongated into an ellipsoidal shape. At this point the bubble either collapsed almost instantly (80°F. stream temperature) or grew slightly larger and collapsed in the center of the vertical dimension, forming a pinched bubble, and then collapsed rapidly (120°F. stream temperature). Through nearly all the bubble lifetime an ellipsoidal shape was a good approximation, while the surface of the bubble was smooth at all times. The frequency of these bubbles was in the range of 2,500 cycles/sec. These bubbles approximated closely the bubbles observed by Gunther in subcooled nucleate boiling.

Group II: Ellipsoidal Bubbles with Irregular Surface

At increased steam flow rates, with the larger orifice, and at a water temperature of 120°F., the bubbles initially had a flattened, ellipsoidal shape. Bubble growth was accompanied by development from an oblate spheroidal to a prolate spheroidal shape. The bubble collapsed rapidly, usually starting at the leading edge and spreading outwards. The frequency was approximately 720 cycles/sec. The surface of these bubbles was irregularly perturbed at all times, based upon light reflectivity.

Group III: Irregular Bubbles That Do Not Completely Collapse

At higher water temperatures (160° to 180°F.) the bubble was quite irregular in shape, and while there were large oscillations in volume, it never completely collapsed. There were considerable variations in shape in this group of bubbles. The bubbles usually started before complete collapse of the previous bubble as a hemispherical shape. The hemisphere in growing elongated to an ellipsoidal shape. As the bubble further enlarged, it either elongated or widened to become almost spherical in shape, depending upon the steam and water flow rates. The nearly spherical shape would then collapse at the bottom, while the elongated bubbles tended to collapse by pinching in the center of the vertical axis. In the latter case the top portion might remain with a new bubble or might separate and float away as it collapsed. The surface of these bubbles was often fairly smooth but nevertheless always distorted. The frequency and characteristic diameter of these bubbles ranged from approximately 200 to 1,000 cycles/sec. and 0.045 to 0.175 in. for stream temperatures of 160° to 180°F.

For all three groups of bubbles the range of the surface heat transfer coefficient was 13,000 to 316,000 B.t.u./(hr.) (sq. ft.) (°F.); the bubble Strouhal number, 0.1 to 7.5; the bubble Reynolds number, 172 to 14,000; the bubble Nusselt number, 398 to 1,485; and the bubble Peclet number, 990 to 35,400. Complete tabular data are on file with the American Documentation Institute.* On dimensional grounds the data may be correlated in the form of a bubble Nusselt number, a Reynolds number, a Prandtl number, and a fourth parameter, the Strouhal number, which is made necessary by the presence of the bubble pulsations:

$$N_s = \frac{v_b}{v_L} \qquad (3)$$

All physical properties were evaluated at the bulk stream temperature. The Prandtl and Reynolds numbers may be combined to give a Peclet number, since the scatter of the data preclude meaningful determination of four empirical constants and the range of Prandtl number variation was insufficient to distinguish Prandtl number effects. The Strouhal number (*11*) enters into the study of periodic wakes, where it is defined as

$$N_s = \frac{D_b}{V_L \tau} \qquad (4)$$

It is seen that this definition is identical with the one used herein. An alternative dimensionless grouping, which may be employed in place of the Strouhal number, is the Fourier number

$$N_F = \frac{\alpha \tau}{D_b^2} \qquad (5)$$

* Tabular material has been deposited as document 6902 with the American Documentation Institute, Photoduplication Service, Library of Congress, Washington 25, D.C., and may be obtained for $5.00 for photoprints or $2.25 for 35-mm. microfilm.

which is the square of the ratio of the bubble boundary-layer thickness to the bubble diameter.

The best fit on a log-log plot for the data was obtained by mean-square error minimization (IBM-650 computer), as shown in Figures 3 and 4. For Group I bubbles the correlating equation is

$$N_{Nu} = 0.000374\ (N_{Pe})^{1.74}\ N_S^{1.5} \quad (6)$$

Eighty per cent of the data points deviate less than 20% from this equation.

For Group II bubbles the equation was

$$N_{Nu} = 21.1\ (N_{Pe})^{0.404}\ N_S^{0.2} \quad (7)$$

Over 90% of the points deviate less than 20% from this equation.

$$N_{Nu} = 63.7\ (N_{Pe})^{0.265}\ N_S^{-0.1} \quad (8)$$

Ninety-seven per cent of the points deviated less than 50% from this equation.

LATENT HEAT TRANSPORT IN SUBCOOLED NUCLEATE BOILING

Gunther (*1*) has made a detailed study of bubble populations in subcooled nucleate boiling of water, using a heated metal strip within a transparent rectangular channel. The system variables were the water velocity and subcooling and the heat flux from the metal surface. By means of high-speed photography of the boiling surface, average values of the maximum bubble radius, the bubble lifetime, and the number of bubbles forming per unit area of surface per unit time were obtained. From these measurements it was possible to calculate the fraction of the surface covered by bubbles at any instant. The range of bubble lifetimes and maximum radii were the same (0.30 to 0.5 msec. and 0.015 to 0.02 in.) as those for Group I bubbles in this study, which were also smooth ellipsoids throughout their lifetime. Using the results of this work one may therefore estimate the heat flux from the surface of the bubbles at any instant in the experiments of reference *1*. This has been done with Equation (6). The results are presented in Figure 5 in the form of ratio Q_L/Q_T. Three sets of runs were reported in which the liquid subcooling, the liquid bulk velocity, and the total heat flux were independently varied. It may be seen from this figure that the latent heat transport is always a significant fraction of the total and is at least an order of magnitude greater than the 1 to 2% previously estimated. As burnout is approached, the importance of this mode of heat transfer increases, and latent heat transport dominates near the maximum heat flux. The latent heat transport is overestimated

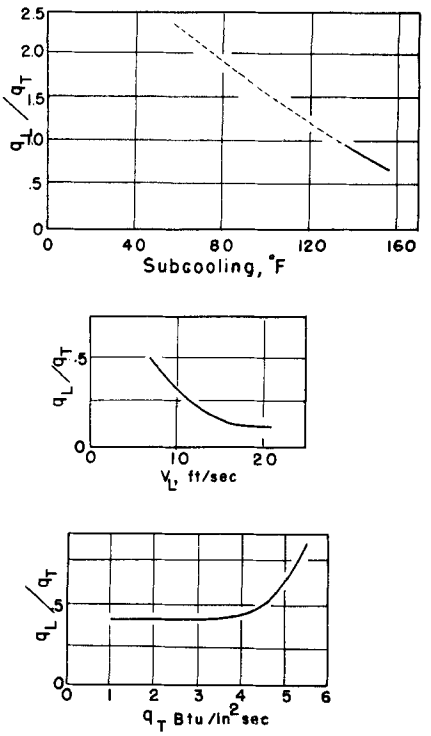

Fig. 5. Estimated fraction of latent heat transport in Gunther's subcooled boiling experiments (*1*), with Group I Equation (6).

at low subcoolings on account of the use of the correlating equation for Group I bubbles, which are small, rapidly growing bubbles associated with high subcoolings. Gunther reported that at low subcoolings the bubbles were larger, more deformed, and tended to detach from the surface.

It should be noted that the geometries in these two sets of experiments were not identical, in one case the flow being parallel to the solid surface and in the other case normal to it. Further, there may be a shielding of one bubble by another in subcooled boiling, which would tend to reduce heat transfer from the bubble surfaces. However this possibility is offset by the reported motion of the bubble along the heating surface at about 0.8 of the free stream velocity. This would produce very significant tangential velocity components, resulting in increased heat transfer from the bubble surface. It appears quite probable therefore that latent heat transport dominates in subcooled nucleate boiling near the maximum heat flux.

ACKNOWLEDGMENT

This work was supported by a National Science Foundation grant. Miss Emily Howland assisted in analysis of the film. Mr. R. C. Kesselring performed the computer correlation.

NOTATION

c_L = liquid surface heat
D_b = diameter of the equivalent sphere
D_t = tube diameter
f = Fanning friction factor
g_c = gravitational conversion factor
h_b = convective heat transfer coefficient from the bubble
k_L = liquid thermal conductivity
N_F = bubble Fourier number, $\alpha\tau/D_b^2$
N_{Nu} = bubble Nusselt number, $h_b D_b/k_L$
N_{Pe} = bubble Peclet number, $D_b v_b \rho_L c_L/k_L$
N_{Re} = bubble Reynolds number, $D_b v_b \rho_L/\mu_L$
N_S = Strouhal number, v_b/v_L
Q_L = latent heat transport rate per unit area of heat surface
Q_T = total heat flux from heating surface
R = radius of the equivalent sphere
v_b = mean bubble wall velocity
v_L = liquid jet velocity
v_S = mean velocity of steam in orifice tube

Greek Letters

α = thermal diffusivity of liquid
ΔP_1 = irreversible pressure loss of steam
ΔP_2 = inertial pressure excess of bubble interior over pressure at infinity
μ = viscosity of water
ρ_L = density of water
ρ_s = density of steam
τ = bubble lifetime

LITERATURE CITED

1. Gunther, F. C., *Progress Report No. 4-75,* Jet Propulsion Laboratory, California Institute of Technology, Pasadena, California (June, 1950).
2. ———, and Frank Kreith, *Progress Report No. 4-120,* Jet Propulsion Laboratory, California Institute of Technology, Pasadena, California (March, 1950).
3. Rohsenow, W. M., and J. A. Clark, *Trans. Am. Soc. Mech. Engrs.,* **73,** 609-20 (1951).
4. Mixon, R. O., Jr., W. Y. Chon, and K. O. Beatty, Jr., *Chem. Eng. Progr. Symposium Series, No. 30,* **56,** 75 (1960).
5. Bankoff, S. G., *ibid., No. 32,* **57,** 156 (Part I) and 164 (Part II) (1961).
6. Frossling, N., *Gerlands Beitrage Geophysik,* **52,** 170 (1938).
7. Kramer, H., *Physics,* **12,** 61 (1946).
8. Maisel, D. S., and T. K. Sherwood, *Chem. Eng. Progr.,* **46,** 131 (1950).
9. Ranz, W. E., and W. R. Marshall, Jr., *ibid.,* **48,** 141 (Part I) and 173 (Part II) (1952).
10. Hsu, N. T., and B. H. Sage, *A.I.Ch.E. Journal,* **3,** 405 (1957).
11. Strouhal, D., *Ann. der Phys. und Chemie,* **5,** 1878; Lord Rayleigh, "Theory of Sound," 2 ed., Vol. 2, chap. 20-21, Macmillan, London, England (1896).

Manuscript received January 26, 1961; revision received June 16, 1961; paper accepted June 16, 1961.